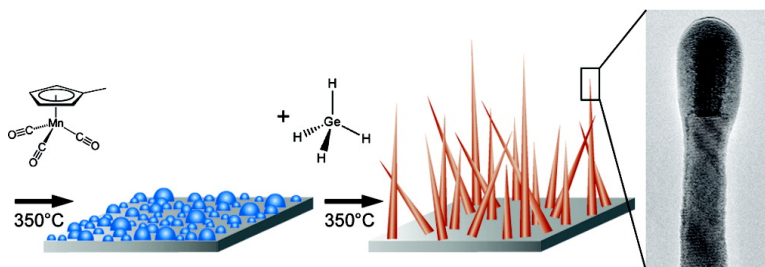


Vapor–Solid–Solid Synthesis of Ge Nanowires from Vapor-Phase-Deposited Manganese Germanide Seeds

Jessica L. Lensch-Falk, Eric R. Hemesath, Francisco J. Lopez, and Lincoln J. Lauhon

J. Am. Chem. Soc., **2007**, 129 (35), 10670-10671 • DOI: 10.1021/ja074276j • Publication Date (Web): 09 August 2007

Downloaded from <http://pubs.acs.org> on February 15, 2009



More About This Article

Additional resources and features associated with this article are available within the HTML version:

- Supporting Information
- Links to the 6 articles that cite this article, as of the time of this article download
- Access to high resolution figures
- Links to articles and content related to this article
- Copyright permission to reproduce figures and/or text from this article

[View the Full Text HTML](#)



Vapor–Solid–Solid Synthesis of Ge Nanowires from Vapor-Phase-Deposited Manganese Germanide Seeds

Jessica L. Lensch-Falk, Eric R. Hemesath, Francisco J. Lopez, and Lincoln J. Lauhon*

Department of Materials Science and Engineering, Northwestern University, Evanston, Illinois 60208-3108

Received June 12, 2007; E-mail: lauho@northwestern.edu

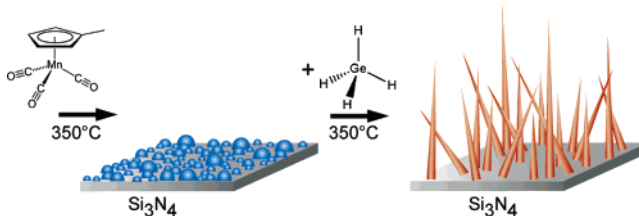
One-dimensional semiconductor materials have been synthesized using a wide range of approaches with various advantages and limitations.^{1,2} Seeded nanowire growth via the vapor–liquid–solid (VLS)³ and vapor–solid–solid (VSS)⁴ mechanisms is broadly exploited to direct the growth of nanowires of controlled morphology and composition.^{3,5} VLS and VSS growth mechanisms are often employed in the context of chemical vapor deposition (CVD), in which reactive gases are selectively decomposed by a metal seed particle. The seed particle is typically deposited in a separate step by methods including metal film evaporation,⁶ gas-phase nanocluster deposition,⁷ and solution-phase deposition of colloidal metal particles.⁸ In comparison, solution–liquid–solid¹ (SLS), supercritical fluid–liquid–solid⁹ (SFLS), and supercritical fluid–solid–solid¹⁰ (SFSS) nanowire growth provide straightforward means to synthesize both seed particles and nanowires sequentially in the same reactor. This advantage is sometimes mitigated, however, by the challenge of controlling the incorporation of intentional impurities, such as dopants, as well as unintentional impurities from the precursors.¹¹

Here we report the sequential synthesis of solid-phase manganese germanide seed particles and crystalline germanium nanowires using low-pressure thermal CVD. This approach to VSS Ge nanowire growth has at least three compelling advantages: (1) the seed particle is not Au, avoiding the potentially negative influence on electrical properties; (2) the vapor-phase deposition and self-assembly of the seed greatly simplifies the nanowire synthesis process; and (3) the self-assembled seed naturally produces a narrow distribution of nanowire diameters.

The sequential synthesis of manganese germanide seeds and Ge nanowires is depicted in Scheme 1. Si₃N₄ substrates were cleaned by sonication in ethanol and loaded into a hot-wall CVD system. Mn was deposited by flowing 20 sccm H₂ through a tricarbonyl-(methylcyclopentadienyl) manganese (TCMn) bubbler, held at 55 °C and 300 Torr, and into the reactor with 30 sccm of N₂ as the dilutant gas. The reactor temperature and pressure were 350 °C and 100 Torr, respectively, and typical deposition times were 5–10 min. These reactor conditions are sufficient to initiate pyrolysis of the TCMn in the gas-phase prior to arrival at the substrate, though pyrolysis is not expected to be complete prior to adsorption of the TCMn decomposition products on the substrate.¹² To complete the decomposition of TCMn and allow Mn nanoparticles to form, the Mn deposition was followed by an anneal in 25 sccm each of N₂/H₂ for 5–15 min. Annealing was found to improve the nanowire yield without influencing the nanowire diameter distribution. The size distribution of the Mn particles formed in this manner was determined *ex situ* using atomic force microscopy (AFM) and threshold height analysis. Figure 1 indicates that the vast majority of particles are below 10 nm in height, but heights up to ~40 nm were observed.

Ge nanowire synthesis was initiated at 350 °C immediately after Mn deposition and annealing by introducing 0.125 sccm GeH₄ along

Scheme 1. Deposition of Mn Seeds by Pyrolysis of TCMn Followed by the Sequential Growth of Ge Nanowires upon Exposure to GeH₄



with 25 sccm each of N₂ and H₂ at a total pressure of 25 Torr. The samples were cooled in the N₂/H₂ mixture. Growths of 15–120 min were subsequently analyzed by scanning electron microscopy (SEM) to determine nanowire lengths and growth rates; Figure 1c shows an SEM image from a 120 min growth with nanowires up to 20 μm in length. The maximum growth rate observed was 190 nm/min, and studies of a series of increasing germane deposition times indicate that a nucleation period of approximately 15 min is required for nanowire growth to begin. Nanowire tip diameters of 10–30 nm were observed with a peak in the distribution of ~18 nm as measured using TEM (Figure 1d).

Elongated “leader” particles were found at the tips of all Ge nanowires (Figure 2a). Analytical and high-resolution TEM was used to further characterize the nanowire and leader structure and composition. High-resolution TEM images show a crystalline core

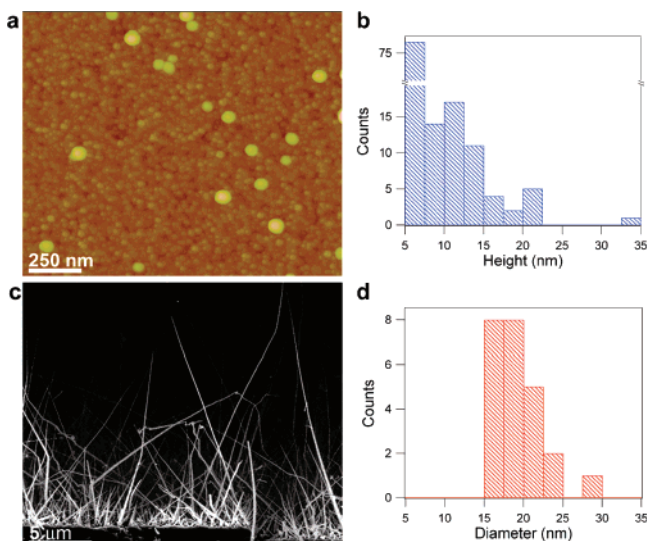


Figure 1. (a) AFM image showing Mn seeds from a 5 min deposition followed by a 15 min anneal on a Si₃N₄ substrate. (b) Histogram of the height distribution for Mn seeds determined using AFM. (c) FE-SEM image of Ge nanowires grown for 120 min. (d) Histogram of the Ge nanowire tip diameters grown from seeds prepared by the same method as (a) (determined using TEM). The distribution of Ge nanowire diameters is narrower than that of the seed particles and peaked at 16–18 nm.

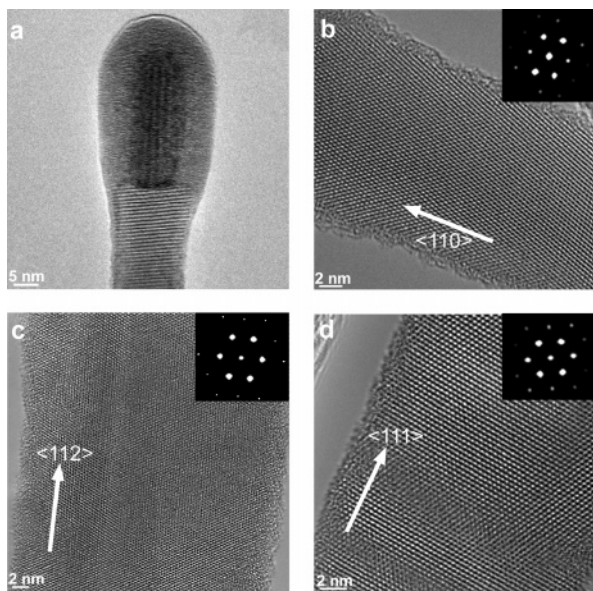


Figure 2. High-resolution TEM images (JEOL JEM-2100F) of the Ge nanowires. (a) An elongated seed particle, or “leader”, is seen at the tip of a Ge nanowire. The crystalline manganese germanide core is surrounded by an amorphous $\text{Mn}_x\text{Ge}_{1-x}$ shell. The Ge-germanide growth interface is abrupt. (b) A 17 nm (diameter) nanowire with $\langle 110 \rangle$ growth axis. (c) A 30 nm nanowire with $\langle 112 \rangle$ growth axis. (d) A 32 nm nanowire with $\langle 111 \rangle$ growth axis. The inset FFTs indicate the growth axes.

with an amorphous shell at the tip of the Mn-seeded nanowires (Figure 2a). Energy dispersive X-ray spectroscopy (Supporting Information) indicates that Mn and Ge are present in both the core and the shell of the leader. The leader shown in Figure 1a is not on a low-index zone axis, but electron diffraction studies of other leaders established the crystalline phase as $\text{Mn}_{11}\text{Ge}_8$ (Supporting Information). HRTEM and diffraction analysis led to the identification of Ge nanowires with $\langle 110 \rangle$, $\langle 111 \rangle$, and $\langle 112 \rangle$ growth directions (Figure 2b–d). A statistical study of the growth axis for ~ 50 nanowires found that 44% are oriented along the $\langle 110 \rangle$ direction, 30% along the $\langle 112 \rangle$ direction, and 26% along the $\langle 111 \rangle$ direction. The dominant orientation is $\langle 110 \rangle$ for tip diameters less than 14 nm, whereas for larger tip diameters, the most prevalent growth direction is $\langle 111 \rangle$. This observed diameter dependence on the nanowire growth axis is reminiscent of reports by Hanrath et al.¹³ for SFLS grown Ge nanowires and by Wu et al.¹⁴ and Schmidt et al.¹⁵ for VLS grown Si nanowires, despite the differences in the growth mechanism. This interesting finding warrants further study, as it has been proposed that a fluctuating liquid–solid interface is responsible for the selectivity.¹⁵

We conclude from the above data that the crystalline “leader” directs crystalline Ge nanowire growth from a gas-phase precursor. The observed nanowire nucleation time of ~ 15 min can be attributed to the formation of the manganese germanide leader from the Mn particles in the presence of GeH_4 . Interestingly, the growth occurs 370 °C below the lowest eutectic point on the Mn–Ge binary phase diagram, suggesting that the leader is solid during this VSS nanowire growth.¹⁶ We have intentionally avoided using the term “catalyst” to refer to the leader because we have not established the extent to which the amorphous $\text{Mn}_x\text{Ge}_{1-x}$ region promotes the decomposition of GeH_4 . Most generally, the leader–nanowire

interface can be understood to lower the energy of formation of the germanium crystal, leading to growth along a particular axis.

A more detailed discussion of this unusual growth process must be deferred, but we can identify the essential elements of one-dimensional growth as (1) a fixed leader diameter and (2) a stable leader morphology at the Ge nanowire tip. As will be described in a future publication, the leader lengthens with time but does not increase in diameter, confirming that the leader is a solid during growth. Ge and Mn adatoms on the tip must therefore diffuse to the leader–nanowire interface, where they incorporate into the crystalline nanowire and leader, respectively, and contribute to elongation. In the absence of continued TCMn flow, the nanowire growth eventually stops. Importantly, it appears that further growth of the crystalline germanide in the radial direction is energetically unfavorable. This observation is certainly related to the narrow range of nanowire tip diameters, which originates from the narrow diameter range of the leader nuclei.

In summary, we report the VSS growth of Ge nanowires with a narrow diameter distribution from CVD-deposited self-assembled manganese seed particles. The similarities between metal germanides, and between germanides and silicides, suggest that this growth mechanism might be extended to other systems including silicon nanowires.

Acknowledgment. This work was supported by the Office of Naval Research, the American Chemical Society Petroleum Research Fund, and the National Science Foundation. J.L.L. acknowledges the support of a NSF Graduate Fellowship, and L.J.L. acknowledges support of an Alfred P. Sloan Research Fellowship. We acknowledge the EPIC facility of NUANCE for use of the microscopy facilities. The NUANCE Center is supported by NSF-NSEC, NSF-MRSEC, Keck Foundation, the State of Illinois, and Northwestern University.

Supporting Information Available: Two figures describing further analysis of the seed particle. This material is available free of charge via the Internet at <http://pubs.acs.org>.

References

- (1) Wang, F. D.; Dong, A. G.; Sun, J. W.; Tang, R.; Yu, H.; Buhro, W. E. *Inorg. Chem.* **2006**, *45*, 7511–7521.
- (2) Xia, Y. N.; Yang, P. D.; Sun, Y. G.; Wu, Y. Y.; Mayers, B.; Gates, B.; Yin, Y. D.; Kim, F.; Yan, Y. Q. *Adv. Mater.* **2003**, *15*, 353–389.
- (3) Wagner, R. S.; Ellis, W. C. *Appl. Phys. Lett.* **1964**, *4*, 89–90.
- (4) Persson, A. I.; Larsson, M. W.; Stenstrom, S.; Ohlsson, B. J.; Samuelson, L.; Wallenberg, L. R. *Nat. Mater.* **2004**, *3*, 677–681.
- (5) Cui, Y.; Lauhon, L. J.; Gudiksen, M. S.; Wang, J. F.; Lieber, C. M. *Appl. Phys. Lett.* **2001**, *78*, 2214–2216.
- (6) Martensson, T.; Borgstrom, M.; Seifert, W.; Ohlsson, B. J.; Samuelson, L. *Nanotechnology* **2003**, *14*, 1255–1258.
- (7) Bjork, M. T.; Ohlsson, B. J.; Sass, T.; Persson, A. I.; Thelander, C.; Magnusson, M. H.; Deppert, K.; Wallenberg, L. R.; Samuelson, L. *Appl. Phys. Lett.* **2002**, *80*, 1058–1060.
- (8) Gudiksen, M. S.; Lieber, C. M. *J. Am. Chem. Soc.* **2000**, *122*, 8801–8802.
- (9) Hanrath, T.; Korgel, B. A. *J. Am. Chem. Soc.* **2002**, *124*, 1424–1429.
- (10) Tuan, H. Y.; Lee, D. C.; Hanrath, T.; Korgel, B. A. *Chem. Mater.* **2005**, *17*, 5705–5711.
- (11) Schrickler, A. D.; Davidson, F. M.; Wiacek, R. J.; Korgel, B. A. *Nanotechnology* **2006**, *17*, 2681–2688.
- (12) Sang, W. B.; Durose, K.; Brinkman, A. W.; Tanner, B. K. *Mater. Chem. Phys.* **1997**, *47*, 75–77.
- (13) Hanrath, T.; Korgel, B. A. *Small* **2005**, *1*, 717–721.
- (14) Wu, Y.; Cui, Y.; Huynh, L.; Barrelet, C. J.; Bell, D. C.; Lieber, C. M. *Nano Lett.* **2004**, *4*, 433–436.
- (15) Schmidt, V.; Senz, S.; Gosele, U. *Nano Lett.* **2005**, *5*, 931–935.
- (16) Okamoto, H. *Desk Handbook: Phase Diagrams for Binary Alloys*; ASM International: Materials Park, OH, 2000.

JA074276J